A WAVELET-BASED SMOOTH VARIABLE STRUCTURE FILTER

William Zhang, S. Andrew Gadsden, and Saeid R. Habibi
Department of Mechanical Engineering
McMaster University
Hamilton, Ontario, Canada, L8S 4L7
zhangw53@mcmaster.ca, gadsden@mcmaster.ca, and habibi@mcmaster.ca

ABSTRACT

For linear and well-defined estimation problems with Gaussian noise, the Kalman filter (KF) yields the best result in terms of estimation accuracy. However, the KF performance degrades and can fail in cases involving large uncertainties such as modeling errors in the estimation process. The smooth variable structure filter (SVSF) is a model-based estimation method built on sliding mode theory with excellent robustness to modeling uncertainties. Wavelet theory has attracted interest as a powerful tool for signal and image processing, and can be used to further improve estimation accuracy. In this paper, a new filtering strategy based on stationary wavelet theory and the smooth variable structure filter is proposed. This strategy, referred to as W-SVSF, is applied on an electrohydrostatic actuator (EHA) for the purposes of state estimation. The results of the W-SVSF are compared with the standard KF, SVSF, and combined W-KF.

1.0 INTRODUCTION

The successful control of a mechanical or electrical system depends on the knowledge of the system states and parameters. Observations of the system are made through the use of sensors that provide measurements which contain information on the variables of interest. Filters are used to remove unwanted components such as noise in an effort to provide an accurate estimate of the states [1]. Advanced filtering and estimation methods are model-based and as such are sensitive to modeling uncertainties. The most popular and well-studied estimation method is the Kalman filter (KF), which was introduced in the 1960s [2,3]. The KF yields a statistically optimal solution for linear estimation problems, as defined by (1.1) and (1.2), in the presence of Gaussian noise where $P(w_k)\sim\mathcal{N}(0,Q_k)$ and $P(v_k)\sim\mathcal{N}(0,R_k)$. A typical model is represented by the following equations:

$$x_{k+1} = Ax_k + Bu_k + w_k \tag{1.1}$$

$$z_{k+1} = Cx_{k+1} + v_{k+1} \tag{1.2}$$

The nomenclature is described and explained throughout this paper. It is the goal of a filter to remove the effects that the system w_k and measurement v_k noise have on extracting the true state values x_k from the measurements z_k. The KF is formulated in a predictor-corrector manner. The states are first estimated using the system model, termed as a priori estimates, meaning ‘prior to’ knowledge of the observations.

A correction term is then added based on the innovation (also called residuals or measurement errors), thus forming the updated or a posteriori (meaning ‘subsequent to’ the observations) state estimates. For linear and well-defined estimation problems with Gaussian white noise, the Kalman filter (KF) yields the best result in terms of estimation accuracy. However, the KF performance degrades and can fail in cases involving large uncertainties such as modeling errors in the estimation process. The smooth variable structure filter (SVSF) is a relatively new estimation strategy based on sliding mode theory, and has been shown to be robust to modeling uncertainties. Similarly to a sliding mode controller (SMC), the SVSF implements a discontinuous switching gain and a smoothing boundary layer ψ. This results in a strategy which is robust to modeling uncertainties and errors.

Wavelet theory has attracted considerable interest as a powerful tool for signal and image processing [4,5]. Wavelets can effectively extract information in both the time and frequency domains, with an adjustable resolution which makes it a powerful tool for the analysis of time-series signals [6]. However, the effectiveness of wavelet theory is even more valuable when used as a pre-processing tool known as multi-scale analysis [7,8]. This technique has been applied to a number of applications, including: estimation [9,10,11], detection [12], classification [12], compression [13], prediction and filtering [14], and synthesis [15]. A number of wavelet-based tools have been proposed: ranging from thresholding wavelet coefficients, to tree-based wavelet de-noising methods.

The combination of wavelet theory with other time-series filtering and estimation approaches have been explored, such as: artificial neural networks [16,17,18], Kalman filtering [6,9,19], and an autoregressive model [20]. Hong [9] utilized the discrete wavelet transform to decompose the state variables of the KF into different components at a desired resolution level. The prediction, correction, and update procedures were modified accordingly based on the decomposed state variables [21]. The algorithm can effectively improve the performance of the KF due to the additional filtering effect from the wavelet [9].

In this paper, a new filtering strategy is proposed by combining a stationary wavelet transform with the SVSF. The additional smoothing function provided by the wavelet effectively reduces the SVSF chattering effect. This improves the overall estimation accuracy, which is useful for control purposes. The results of applying the KF, SVSF, W-KF, and W-SVSF on an electrohydrostatic actuator (EHA) are compared and discussed.

2.0 WAVELET THEORY

2.1 Introduction

A discrete wavelet transform (DWT) is similar to a Fourier transform. However, the wavelet transform is considered to be more flexible and informative [21]. By applying a DWT to a time series signal, one may decompose the original signal into different scales, similar to a frequency spectrum [23]. However, unlike a Fourier transform, the DWT has individual wavelet functions localized in space. This localization feature makes many functions and operators using wavelets 'sparse' when transformed into the wavelet domain [24]. This sparseness, in turn, facilitates the process of signal de-noising. The wavelet transform has numerous attractive properties which make it a good signal and image processing technique. These may be summarized as follows [25]:

Locality: Each wavelet is localized simultaneously in time and frequency.

Multi-resolution: Each wavelet is compressed and dilated, and is analyzed at a nested set of scales.

Compression: The wavelet transformations of real-world signals tend to be sparse.

All of these properties enable the wavelet transform to efficiently match a wide range of signal characteristics; from high-frequency transients and edges, to slowly varying harmonics [25].

2.2 Stationary Wavelet Transform

The discrete wavelet transform (DWT) with a thresholding approach has attracted considerable interest for signal and image de-noising [1]. However, a drawback the classical DWT suffers is the time-invariance (a.k.a. pseudo-Gibbs phenomena [2]). That means the DWT of a time-shifted version of a signal is not the translated version of the DWT of the original one.

However, this property is desirable if the wavelet transform is applied for online estimation in a recursive form. One method to suppress such artifacts and restore the translation invariance property is the stationary wavelet transform (SWT) [2,3,4]. The basic concept of the SWT is to apply a shifted DWT without decimation by computing coefficients with up-sampled high-pass and low-pass filters. This occurs for every possible sequence ε at each decimation step j, so that the two new sequences each have the same length as the original sequence. An inverse stationary wavelet transform (ISTW) is then performed by calculating the average of the inverses obtained for every ε-decimated DWT. The wavelet de-noising process includes three main steps: decomposition of time-domain signal, thresholding, and reconstruction of the original data.

Suppose that $\underline{X}_k^N = [x_k^N, x_{k-1}^N, \ \ldots, x_{k-L+1}^N]$ represent a time series of real-valued signals at scale N with minimum dyadic length $L = 2^N$, where $N = 0,1, \ldots J$ and J is the total decomposition level. $W_{k_D}^N$ and $W_{k_A}^N$ are vectors of the details and approximations of SWT respectively, with $\underline{X}_k^0$ defined as the original signal. This then yields:

$$W_{k_D}^{N+1} = F^N W_{k_A}^N \tag{2.1}$$

$$W_{k_A}^{N+1} = G^N W_{k_A}^N \tag{2.2}$$

As shown in Fig. 1, the operators F^N and G^N represent low-pass and high-pass filters, respectively. These are obtained by upsampling the corresponding filters of the previous level.

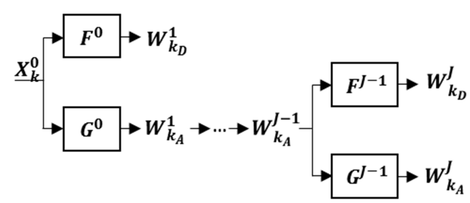

FIGURE 1. ILLUSTRATION OF A WAVELET TRANSFORM

Suppose that the wavelet transform operation is defined as T, then the transformed matrix is obtained as: $W_{(J+1)\times L,k} = T\underline{X}_k^0 = [W_{k_D}^1, \ldots, W_{k_D}^J, W_{k_A}^J]^T$. The universal threshold $\sqrt{2log(n)}\hat{\sigma}$ is calculated based on offline data [1] and applied to $W_{(J+1)\times L,k}$ for suppressing noise-induced spikes that spoil the smoothness of reconstructions. As a preliminary example, a two level Haar wavelet is chosen to demonstrate the effectiveness of this filtering scheme.

3.0 ESTIMATION THEORY

3.1 Kalman Filter

The KF has been broadly applied to problems covering state and parameter estimation, signal processing, target tracking, fault detection and diagnosis, and even financial analysis [4,5]. The success of the KF comes from the optimality of the Kalman gain in minimizing the trace of the a posteriori state error covariance matrix [6,7]. The trace is taken because it represents the state error vector in the estimation process [8]. The following five equations form the core of the KF algorithm, and are used in an iterative fashion. Equations (1.3) and (1.4) define the a priori state estimate $\hat{x}_{k+1|k}$ based on knowledge of the linear system A, the previous state estimate $\hat{x}_{k|k}$, the input matrix B, the input u_k, and the corresponding state error covariance matrix $P_{k+1|k}$, respectively.

$$\hat{x}_{k+1|k} = A\hat{x}_{k|k} + Bu_k \tag{3.1.1}$$

$$P_{k+1|k} = AP_{k|k}A^T + Q_k \tag{3.1.2}$$

The Kalman gain K_{k+1} is defined by (1.5), and is used to update the state estimate $\hat{x}_{k+1|k+1}$ as shown in (1.6). The gain makes use of an innovation covariance S_{k+1}, which is defined as the inverse term found in (1.5).

$$K_{k+1} = P_{k+1|k}C^T\left[CP_{k+1|k}C^T + R_{k+1}\right]^{-1} \tag{3.1.3}$$

$$\hat{x}_{k+1|k+1} = \hat{x}_{k+1|k} + K_{k+1}\left[z_{k+1} - C\hat{x}_{k+1|k}\right] \tag{3.1.4}$$

The a posteriori state error covariance matrix $P_{k+1|k+1}$ is then calculated by (1.7), and is used iteratively, as per (1.4).

$$P_{k+1|k+1} = [I - K_{k+1}C]P_{k+1|k} \tag{3.1.5}$$

A number of different methods have extended the classical KF to nonlinear systems, with the most popular and simplest method being the extended Kalman filter (EKF) [9,10]. The EKF is conceptually similar to the KF; however, the nonlinear system is linearized according to its Jacobian. This linearization process introduces uncertainties that can sometimes cause instability [10].

3.2 Smooth Variable Structure Filter

The smooth variable structure filter (SVSF) was presented in 2007 [28]. The SVSF strategy is a predictor-corrector estimator based on sliding mode concepts, and can be applied on both linear or nonlinear systems and measurements. As shown in Fig. 2, it utilizes a switching gain to converge the estimates to within a boundary of the true state values (i.e., existence subspace) [28]. The SVSF has been shown to be stable and robust to modeling uncertainties and noise, when given an upper bound on the level of unmodeled dynamics and noise [28,21]. The origin of the SVSF name comes from the requirement that the system is differentiable (or 'smooth') [28,29]. Furthermore, it is assumed that the system under consideration is observable [28].

Consider the following process for the SVSF estimation strategy, as applied to a linear system with a linear measurement equation. Note that this formulation includes state error covariance equations as presented in [30], which was not originally presented in the standard SVSF form [28]. The predicted state estimates $\hat{x}_{k+1|k}$ are first calculated as follows:

$$\hat{x}_{k+1|k} = A\hat{x}_{k|k} + Bu_k \tag{3.2.1}$$

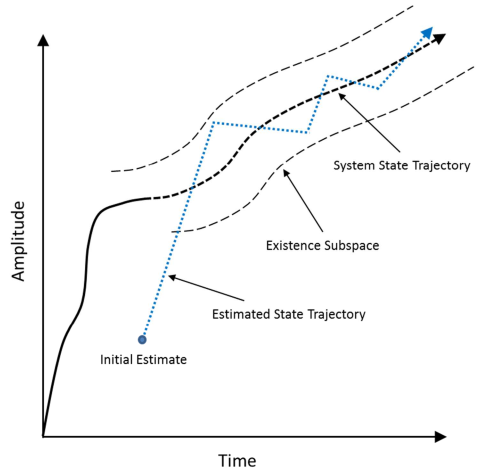

FIGURE 2. SVSF ESTIMATION CONCEPT [30]

Similar to the KF, the a priori state error covariance matrix $P_{k+1|k}$ may be found as follows:

$$P_{k+1|k} = AP_{k|k}A^T + Q_k \tag{3.2.2}$$

Utilizing the predicted state estimates $\hat{x}_{k+1|k}$, the corresponding predicted measurements $\hat{z}_{k+1|k}$ and error vector $e_{z,k+1|k}$ may be calculated:

$$\hat{z}_{k+1|k} = C\hat{x}_{k+1|k} \tag{3.2.3}$$

$$e_{z,k+1|k} = z_{k+1} - \hat{z}_{k+1|k} \tag{3.2.4}$$

Next, the SVSF gain is calculated as follows [6]:

$$\begin{aligned} K_{k+1} &= C^+ diag\left[\left(\left|e_{z,k+1|k}\right|_{Abs} + \gamma\left|e_{z,k|k}\right|_{Abs}\right)\right. \\ &\left.\circ\, sat\left(\frac{e_{z,k+1|k}}{\psi_i}\right)\right]\left[diag\left(e_{z,k+1|k}\right)\right]^{-1} \end{aligned} \tag{3.2.5}$$

The SVSF gain is a function of: the a priori and a posteriori measurement error vectors $e_{z,k+1|k}$ and $e_{z,k|k}$; the smoothing boundary layer widths ψ_i where i refers to the i^{th} width; the 'SVSF' memory or convergence rate γ with elements $0 < \gamma_{ii} \leq 1$; and the linear measurement matrix C. However, for numerical stability, it is important to ensure that one does not divide by zero in (3.2.5). This can be accomplished using a simple if statement with a very small threshold (i.e., 1×10^{-12}). The SVSF gain is used to refine the state estimates as follows:

$$\hat{x}_{k+1|k+1} = \hat{x}_{k+1|k} + K_{k+1}e_{z,k+1|k} \tag{3.2.6}$$

Following this, the a posteriori state error covariance matrix $P_{k+1|k+1}$ is calculated as follows [6]:

$$\begin{aligned} P_{k+1|k+1} = (I - K_{k+1}C)P_{k+1|k}(I - K_{k+1}C)^T \\ + K_{k+1}R_{k+1}K_{k+1}^T \end{aligned} \tag{3.2.7}$$

Next, the updated measurement estimates $\hat{z}_{k+1|k+1}$ and corresponding errors $e_{z,k+1|k+1}$ are calculated:

$$\hat{z}_{k+1|k+1} = C\hat{x}_{k+1|k+1} \tag{3.2.8}$$

$$e_{z,k+1|k+1} = z_{k+1} - \hat{z}_{k+1|k+1} \tag{3.2.9}$$

The SVSF process may be summarized by (3.2.1) through (3.2.9), and is repeated iteratively. According to [28], the estimation process is stable and converges to the existence subspace if the following condition is satisfied:

$$\left|e_{k|k}\right|_{Abs} > \left|e_{k+1|k+1}\right|_{Abs} \tag{3.2.10}$$

Note that $|e|_{Abs}$ is the absolute of the vector e, and is equal to $|e|_{Abs} = e \cdot sign(e)$. The proof, as described in [28] and [29], yields the derivation of the SVSF gain from (2.8). The SVSF results in the state estimates converging to within a region of the state trajectory, referred to as the existence subspace. Thereafter, it switches back and forth across the state trajectory, as shown earlier in Fig. 2. The existence subspace shown in Fig. 2 represents the amount of uncertainties present in the estimation process, in terms of modeling errors or the presence of noise. The width of the existence space β is a function of the uncertain dynamics associated with the inaccuracy of the internal model of the filter as well as the measurement model, and varies with time [28]. Typically this value is not exactly known but an upper bound may be selected based on a priori knowledge.

Once within the existence boundary subspace, the estimated states are forced (by the SVSF gain) to switch back and forth along the true state trajectory. As mentioned earlier, high-frequency switching caused by the SVSF gain is referred to as chattering, and in most cases, is undesirable for obtaining accurate estimates [28]. However, the effects of chattering may be minimized by the introduction of a smoothing boundary layer ψ. The selection of the smoothing boundary layer width reflects the level of uncertainties in the filter and the disturbances (i.e., system and measurement noise, and unmodeled dynamics). When the smoothing boundary layer is defined larger than the existence subspace boundary, the estimated state trajectory is smoothed. However, when the smoothing term is too small, chattering remains due to the uncertainties being underestimated.

4.0 PROPOSED W-SVSF ESTIMATION STRATEGY

The W-SVSF estimation strategy proposed in this paper may be summarized by the following sets of equations. The state estimates $\hat{x}_{k+1|k}$, error covariance $P_{k+1|k}$, and measurement errors $e_{z,k+1|k}$ are first predicted as follows:

$$\hat{x}_{k+1|k} = A\hat{x}_{k|k} + Bu_k \tag{4.1}$$

$$P_{k+1|k} = AP_{k|k}A^T + Q_k \tag{4.2}$$

$$e_{z,k+1|k} = z_{k+1} - C\hat{x}_{k+1|k} \tag{4.3}$$

Next, the SVSF gain K_{k+1} is calculated as follows:

$$\begin{aligned} &K_{k+1} \\ &= C^+ diag\left[\left(\left|e_{z,k+1|k}\right|_{Abs} + \gamma\left|e_{z,k|k}\right|_{Abs}\right) \right. \\ &\left. \circ\, sat\left(\frac{e_{z,k+1|k}}{\psi_i}\right)\right]\left[diag\left(e_{z,k+1|k}\right)\right]^{-1} \end{aligned} \tag{4.4}$$

The SVSF gain is used to refine the state estimates $\hat{x}_{k+1|k+1}$ and state error covariance $P_{k+1|k+1}$ as follows:

$$\hat{x}_{k+1|k+1} = \hat{x}_{k+1|k} + K_{k+1}e_{z,k+1|k} \tag{4.5}$$

$$\begin{aligned} P_{k+1|k+1} = (I - K_{k+1}C)P_{k+1|k}(I - K_{k+1}C)^T \\ + K_{k+1}R_{k+1}K_{k+1}^T \end{aligned} \tag{4.6}$$

The wavelet vectors $W_{(J+1)\times L,k}$ are then created by transforming the updated state estimates (4.5) as follows:

$$W_{(J+1)\times L,k} = T\hat{x}_{k+1|k+1} \tag{4.7}$$

A hard-thresholding function defined by (4.8) is then applied on (4.7) as shown in (4.9):

$$D(x) = \begin{cases} 1 & if|x| \geq thr \\ 0 & if|x| < thr \end{cases} \tag{4.8}$$

$$W_{(J+1)\times L,k}^d = D(W_{(J+1)\times L,k}) \tag{4.9}$$

The original data is reconstructed yielding the final updated state estimates:

$$\hat{x}_{k+1|k+1} = T^{-1}W_{(J+1)\times L,k}^d \tag{4.10}$$

Finally, the measurement errors $e_{z,k+1|k+1}$ are also updated:

$$e_{z,k+1|k+1} = z_{k+1} - C\hat{x}_{k+1|k+1} \tag{4.11}$$

Note that the W-KF strategy is similar to the above W-SVSF method, except that the gain formulation (4.4) is different, as defined by (3.1.3).

5.0 COMPUTER EXPERIMENT

5.1 Problem Description and Setup

In this section, the proposed estimation strategy is applied for the purposes of state estimation on an electrohydrostatic actuator (EHA). This example uses computer simulations in order to allow a detailed investigation of the effects of parametric uncertainties. The EHA model is based on an actual prototype built for experimentation [28,34]. The purpose of this example is to demonstrate that the W-SVSF estimation process is functional, and that the resulting estimation process demonstrates improvements over the KF, W-KF, and SVSF. Furthermore, the addition of modeling errors will demonstrate its robustness. For this computer experiment, the input to the system is a random signal with amplitude in the range of $\pm 1\ rad/s$, superimposed onto a unit step occurring at 0.5 s, as shown in Fig. 3.

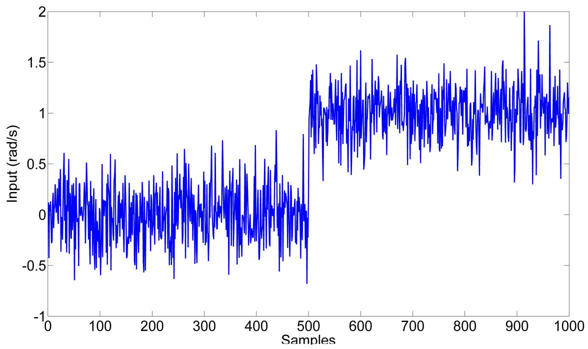

FIGURE 3. INPUT SIGNAL

The EHA has been modeled as a third-order linear system with state variables related to its position, velocity, and acceleration [28]. Initially, it is assumed that the first two states have measurements associated with them, and the acceleration is not measured. The sample time of the system is $T = 0.001\ s$, and the discrete-time state space system equation may be defined as follows [28]:

$$x_{k+1} = \begin{bmatrix} 1 & 0.001 & 0 \\ 0 & 1 & 0.001 \\ -557.02 & -28.616 & 0.9418 \end{bmatrix} x_k + \begin{bmatrix} 0 \\ 0 \\ 557.02 \end{bmatrix} u_k \tag{5.1}$$

The corresponding measurement equation is defined by:

$$z_{k+1} = \begin{bmatrix} 1 & 0 & 0 \\ 0 & 1 & 0 \end{bmatrix} x_{k+1} \tag{5.2}$$

The initial state values are set to zero. The system and measurement noises (w and v) are considered to be Gaussian, with zero mean and variances Q and R, respectively. The maximum amplitude of the system and measurement noises are $W_{Max} = [0.01 \quad 1 \quad 10]^T$ and $V_{Max} = [1 \times 10^{-3} \quad 1]^T$, respectively. The initial state error covariance $P_{0|0}$, system noise covariance Q, and measurement noise covariance R are defined respectively as follows:

$$P_{0|0} = 10Q \tag{5.3}$$

$$Q = \begin{bmatrix} 1 \times 10^{-4} & 0 & 0 \\ 0 & 1 \times 10^{-2} & 0 \\ 0 & 0 & 1 \times 10^{3} \end{bmatrix} \tag{5.4}$$

$$R = \begin{bmatrix} 1 \times 10^{-3} & 0 \\ 0 & 1 \times 10^{-1} \end{bmatrix} \tag{5.5}$$

In this example, to demonstrate the robustness of the SVSF and W-SVSF, modeling uncertainty is injected into the estimation process at 0.5 seconds. The system model $\hat{A}$ in (5.1) is modified at this time, such that:

$$\hat{A}_{T=0.5} = \begin{bmatrix} 1 & 0.001 & 0 \\ 0 & 1 & 0.001 \\ -240 & -28 & 0.9418 \end{bmatrix} \tag{5.6}$$

For the standard SVSF estimation process, the 'memory' or convergence rate was set to $\gamma = 0.1$, and the limits for the smoothing boundary layer widths were defined as $\psi = [0.1 \quad 10 \quad 100]^T$. These parameters were selected based on the distribution of the system and measurement noises. For example, the limit for the smoothing boundary layer width ψ was set to 10 times the maximum system noise, or approximately equal to the measurement noise. The initial state estimates for the filters were defined randomly by a normal distribution, around the true initial state values x_0 and using the initial state error covariance $P_{0|0}$.

5.2 Results and Discussion

The state estimation results are shown in Figs. 4 through 6. When the system is operating normally and is well-defined, all four filters perform relatively well; with the KF and W-KF performing the best. However, a noticeable different occurs when modeling uncertainty is injected halfway-through. As demonstrated in the following figures, the SVSF and W-SVSF strategies are both able to stay within a region of the true state trajectory. This leads to a robust method. The addition of the wavelet theory to the SVSF reduces the magnitude of the chattering effect of the SVSF. This improves the overall estimation accuracy, leading to a smoother control signal.

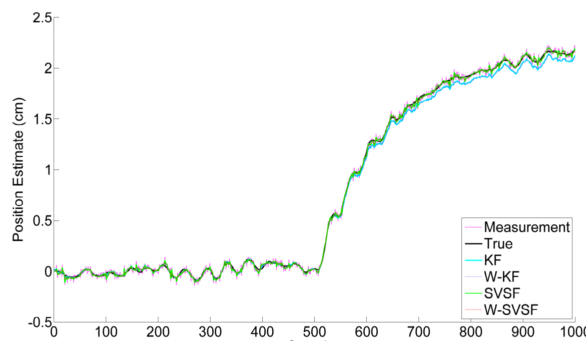

FIGURE 4. RESULTS FOR POSITION ESTIMATES

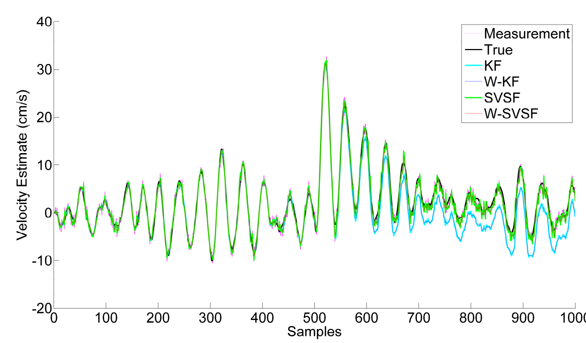

FIGURE 5. RESULTS FOR VELOCITY ESTIMATES

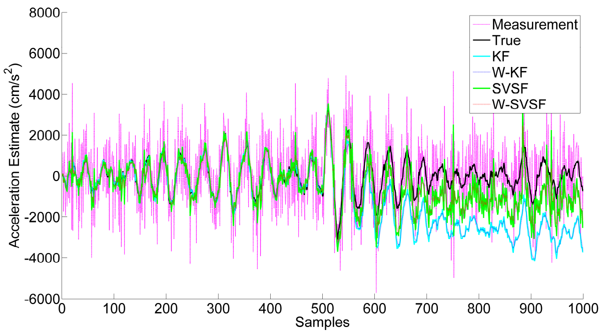

FIGURE 6. RESULTS FOR ACCELERATION ESTIMATES

The root mean square error (RMSE) results are shown in Fig. 7. Note that a set of 200 Monte Carlo simulations were run and the results were averaged. Furthermore, note that K refers to the KF, W-K refers to the W-KF, S refers to the SVSF, and W-S refers to the W-SVSF.

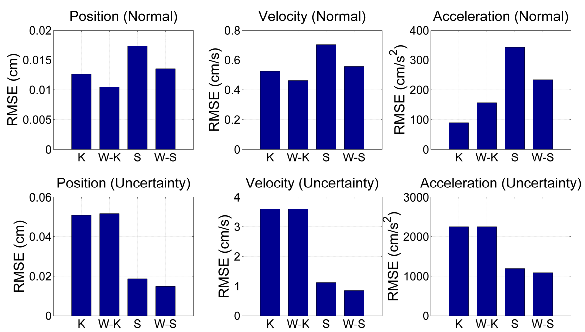

FIGURE 7. RMSE RESULTS (BOTH CASES)

As demonstrated by the above results, the W-SVSF improved the overall estimation accuracy of the standard SVSF by a significant amount ($10 - 25\%$). The W-SVSF estimation method yielded relatively good estimates under normal conditions and the best estimates when modeling uncertainty was present in the system.

6.0 CONCLUSIONS

In this paper, a new filtering strategy was proposed by combining a stationary wavelet transform with the relatively new smooth variable structure filter (SVSF). The additional smoothing function provided by the wavelet effectively reduced the SVSF chattering effect. This improved the overall estimation accuracy, which is useful for control purposes. The results of applying the KF, SVSF, W-KF, and W-SVSF on an electrohydrostatic actuator (EHA) were compared and discussed. The addition of the wavelet transform to the SVSF was found to increase the estimation accuracy by $10 - 25\%$. Future work involves studying new forms of wavelet theory, and implementing these methods on mechanical and electrical systems for the purposes of fault detection and diagnosis.

7.0 REFERENCES

[1] N. Nise, *Control Systems Engineering*, 4th ed. New York: John Wiley and Sons, Inc., 2004.

[2] R. E. Kalman, "A New Approach to Linear Filtering and Prediction Problems," *Journal of Basic Engineering, Transactions of ASME*, vol. 82, pp. 35-45, 1960.

[3] B. D. O. Anderson and J. B. Moore, *Optimal Filtering*. Englewood Cliffs, NJ: Prentice-Hall, 1979.

[4] A. Tangborn and S. Q. Zhang, "Wavelet transform adapted to an approximate Kalman filter system," *Applied Numerical Mathematics*, vol. 33, no. 1-4, pp. 307-316, May 2000.

[5] T. Zheng, A. A. Girgis, and E. B. Makram, "A hybrid wavelet-Kalman filter method for load forecasting," *Electric Power Systems Research*, vol. 54, no. 1, pp. 11-17, April 2000.

[6] Olivier Renaud, Jean-luc Starck, and Fionn Murtagh, "Wavelet-Based Combined Signal Filtering and Prediction," *Methodology & Data Anal.*, vol. 35, pp. 1241-1251 , Dec 2005.

[7] B.-S. Chen and W.-S. Hou, "Deconvolution filter design for fractal signal transmission systems: a multiscale Kalman filter bank approach," *IEEE Transactions on Signal Processing*, pp. 1359 - 1364, May 1997.

[8] K. Chou, A. Willsky, and R. Nikoukhah, "Multiscale systems, Kalman filters, and Riccati equations," *Automatic Control, IEEE Transactions*, vol. 39, no. 3, pp. 479 - 492, March 1994.

[9] L. Hong, G. Cheng, and C.K. Chui, "A filter-bank-based Kalman filtering technique for wavelet estimation and decomposition of random signals," *Circuits and Systems II: Analog and Digital Signal Processing, IEEE Transactions on*, vol. 45, no. 2, pp. 237 - 241, Feb 1998.

[10] J.-C. Pesquet, H. Krim, and E. Hamman, "Bayesian approach to best basis selection," *IEEE Int. Conf. Acoust., Speech, Signal Process ICASSP, Atlanta, GA*, pp. 2634–2637, 1996.

[11] H. Chipman, E. Kolaczyk, and R. McCulloch, "Adaptive Bayesian wavelet shrinkage," *J. Amer. Stat. Assoc.*, vol. 92, 1997.

[12] N. Lee, Q. Huynh, and S. Schwarz, "New methods of linear time-frequency analysis for signal detection," *Proc. IEEE Int. Symp. Time–Freq. Time-Scale Anal.*, 1996.

[13] J. Shapiro, "Embedded image coding using zerotrees of wavelet coefficients," *IEEE Trans. Signal Processing*, vol. 41, pp. 3445–3462, Dec 1993.

[14] Basseville, M.; Benveniste, A.; Kenneth, C. C.; Golden, S. A.; Nikoukhah, R.; Willsky, A. S., "Modeling and Estimation of Multiresolution Stochastic Processes," *IEEE Trans. Information Theory*, vol. 38, pp. 766–784, March 1992.

[15] P. Flandrin, "Wavelet analysis and synthesis of fractional Brownian motion," *IEEE Trans. Inform. Theory*, vol. 38, pp. 910–916, March 1992.

[16] G. Zheng, J.-L. Starck, J. Campbell, and F. Murtagh, "The wavelet transform for filtering financial data streams," *Journal of Computational Intelligence in Finance*, vol. 7(3), pp. 18–35, 1999.

[17] Z. Bashir and M.E. El-Hawary, "Short term load forecasting by using wavelet neural networks," *In Canadian Conference on Electrical and Computer Engineering*, pp. 163–166, 2000.

[18] U. Lotric, "Wavelet based denoising integrated into multilayered perceptron," *Neurocomputing*, vol. 62, pp. 179–196, 2004.

[19] Roberto Cristi and Murali Tummala, "Multirate, multiresolution, recursive Kalman filter," *Signal Processing*, vol. 80, pp. 1945–1958, 2000.

[20] S. Soltani, P. Simard D. Boichu, and S. Canu., "The longterm memory prediction by multiscale decomposition," *Signal Processing*, vol. 80, pp. 2195–2205, 2000.

[21] Chien-Ming Chou and Ru-Yih Wang, "Application of Wavelet-based Multi-model Kalman Filters to Real-time Flood Forecasting," *Hydrol. Process*, vol. 18, pp. 987-1008, 2004.

[22] G. Stephanopoulos, O. Karsligi, and M. Dyer, "Multi-scale aspects in model-predictive control," *Journal of Process Control*, vol. 10, no. 2-3,

pp. 275-282, April 2000.

[23] A. Graps, "An introduction to wavelets," *Computational Science & Engineering, IEEE*, vol. 2, no. 2, pp. 50 - 61, 1995.

[24] Crouse, M.S.; Nowak, R.D.; Baraniuk, R.G., "Wavelet-based statistical signal processing using hidden Markov models," *Signal Processing, IEEE Transactions on*, vol. 46, no. 4, pp. 886 - 902, Apr 1998.

[25] Donald B. Percival and Andrew T. Walden, *Wavelet Methods for Time Series Analysis*. New York: Cambridge University Press, 2000.

[26] R.R. Coifman and D.L. Donoho, "Translation-Invariant De-Noising," 1995.

[27] B. Ristic, S. Arulampalam, and N. Gordon, *Beyond the Kalman Filter: Particle Filters for Tracking Applications*. Boston: Artech House, 2004.

[28] Simon Haykin, *Kalman Filtering and Neural Networks*. New York, U.S.A.: John Wiley and Sons, Inc., 2001.

[29] S. A. Gadsden, "Smooth Variable Structure Filtering: Theory and Applications," Department of Mechanical Engineering, McMaster University, Hamilton, Ontario, Ph.D. Thesis 2011.

[30] S. A. Gadsden, M. Al-Shabi, and S. R. Habibi, "Estimation Strategies for the Condition Monitoring of a Battery System in a Hybrid Electric Vehicle," *ISRN Signal Processing*, 2011.

[31] A. Gelb, *Applied Optimal Estimation*. Cambridge, MA: MIT Press, 1974.

[32] D. Simon, *Optimal State Estimation: Kalman, H-Infinity, and Nonlinear Approaches*.: Wiley-Interscience, 2006.

[33] G. Welch and G. Bishop, "An Introduction to the Kalman Filter," Department of Computer Science, University of North Carolina, 2006.

[34] S. R. Habibi, "The Smooth Variable Structure Filter," *Proceedings of the IEEE*, vol. 95, no. 5, pp. 1026-1059, 2007.

[35] S. R. Habibi and R. Burton, "The Variable Structure Filter," *Journal of Dynamic Systems, Measurement, and Control (ASME)*, vol. 125, pp. 287-293, September 2003.

[36] M. Al-Shabi, "The General Toeplitz/Observability SVSF," Department of Mechanical Engineering, McMaster University, Hamilton, Ontario, Ph.D. Thesis 2011.

[37] S. A. Gadsden and S. R. Habibi, "A New Form of the Smooth Variable Structure Filter with a Covariance Derivation," in *IEEE Conference on Decision and Control*, Atlanta, Georgia, 2010.

[38] S. R. Habibi and R. Burton, "Parameter Identification for a High Performance Hydrostatic Actuation System using the Variable Structure Filter Concept," *ASME Journal of Dynamic Systems, Measurement, and Control*, 2007.